HOKKAIDO UNIVERSITY

Title	Novel Fluorescence-Based Method To Characterize the Antioxidative Effects of Food Metabolites on Lipid Droplets in Cultured Hepatocytes
Author(s)	Tsukui, Takayuki; Chen, Zhen; Fuda, Hirotoshi; Furukawa, Takayuki; Oura, Kotaro; Sakurai, Toshihiro; Hui, Shu-Ping; Chiba, Hitoshi
Citation	Journal of Agricultural and Food Chemistry, 67(35), 9934-9941 https://doi.org/10.1021/acs.jafc.9b02081
Issue Date	2019-08-11
Doc URL	http://hdl.handle.net/2115/79057
Rights	This document is the Accepted Manuscript version of a Published Work that appeared in final form in J. Agric. Food Chem., copyright © American Chemical Society after peer review and technical editing by the publisher. To access the final edited and published work see https://pubs.acs.org/doi/10.1021/acs.jafc.9b02081.
Type	article (author version)
File Information	2019_67(35).pdf

Instructions for use

Hokkaido University Collection of Scholarly and Academic Papers : HUSCAP

Novel fluorescence-based method to characterize the antioxidative effects of food metabolites on lipid droplets in cultured hepatocytes

Takayuki Tsukui[1], Zhen Chen[2], Hirotoshi Fuda[2], Takayuki Furukawa[2], Kotaro Oura[2], Toshihiro Sakurai[2], Shu-Ping Hui[2*], Hitoshi Chiba[1]

1. Department of Nutrition, Sapporo University of Health Sciences, Nakanuma Nishi-4-3-1-15, Higashi-ku, Sapporo 007-0894, Japan
2. Faculty of Health Sciences, Hokkaido University, Kita-12, Nishi-5, Kita-ku, Sapporo 060-0812, Japan

* Correspondence: Shu-Ping Hui. Faculty of Health Sciences, Hokkaido University, Kita-12, Nishi-5, Kita-ku, Sapporo 060-0812, Japan. E-mail: keino@hs.hokudai.ac.jp, Tel. & Fax: +81-11-706-3693.

Abstract

A fluorescence microscopic method for characterizing size, quantity, and oxidation of lipid droplets (LDs) in HepG2 cells was developed. LDs were induced by palmitic (PA), oleic (OA), or linoleic acids (LA), and stained with two fluorescent probes for neutral lipids and lipid peroxides. Each fatty acid increased the number of LDs and oxidized LDs (oxLDs) and the degree of LD oxidation time-dependently, as well as increased intracellular triglyceride hydroperoxides. LDs induced by LA without AAPH showed the most significant oxidation degree over PA and OA, especially in large LDs (area ≥3 μm^2, oxLD/LD = 52.3±21.7%). Under this condition, two food-derived antioxidants were evaluated, and both of them significantly improved the LD characteristics. Moreover, chlorogenic acid reduced the quantity of large LDs by 74.0%−87.6% dose-dependently. The proposed method might provide a new approach to evaluate the effect of dietary antioxidants.

Keywords

Lipid droplet (LD), fluorescence microscopy, antioxidant, lipid oxidation, non-alcoholic fatty liver disease (NAFLD)

1. Introduction

Lipid droplets (LDs) are usually filled with triglyceride (TG) as their hydrophobic cores, and enclosed by a phospholipid monolayer as their hydrophilic shell, which mainly consists of phosphatidylcholine (PC).[1] It is known that LDs are induced by the accumulation of TG in the bilayer membrane of the endoplasmic reticulum.[2] LDs can grow by fusion, ester translocation, and neosynthesis *in situ*,[3–5] resulting in a variety of size distribution. Conventionally, LDs were recognized just as the inert storage for energy. However, in recent years they have been uncovered to be a highly dynamic organelle that plays a central role in lipid and energy homeostasis.[6,7]

In the current researches, the LD imaging by oil red O staining is generally used for lipid accumulation measurement,[8] but the available information is rather limited. A very recent study by Zhao et al. analyzed the profiling of PCs and TGs in the LD of HepG2 cells by in-tip solvent microextraction mass spectrometry (ITSME-MS).[9] However, since that strategy focused on single LD analysis, rather than the whole LDs in the cells, the overall characteristics of LDs in the cells was unavailable, such as their total quantity, their morphology, and their size distribution. Moreover, although the composition of lipid molecular species in LD could be known by MS, there is a lack of information on the oxidized lipids (i.e. lipid oxidation products) in these LDs so far. Therefore, a

comprehensive profiling method for all the LDs in the cells, including multiple index such as quantity, morphology, size, and oxidation degree, is to be established.

It is of great importance to focus on the oxidation in LD, because the oxidized products in LDs can reflect the oxidative stress in the whole cell. More interestingly, it is reported that an increase of reactive oxygen species (ROS) is positively correlated with an increase in the number of LDs in hepatocytes.[10] These changes will lead to the dysfunction of LD homeostasis, which is considered to be a factor causing a series of metabolic syndromes, e.g. obesity and non-alcoholic fatty liver disease (NAFLD).[11–13] ROS is also known to react with the intracellular polyunsaturated fatty acids (PUFAs) and cause lipid peroxidation in the liver of NAFLD patients.[14] Moreover, microvesicular and macrovesicular steatoses are different in prognosis, suggesting a possible relationship between oxidation and size of LDs.[15] Thus, to get a better understanding toward the pathophysiological conditions associated with LDs, detailed investigation on the physicochemical properties of the intact and oxidized LDs is desired.[15]

Researchers have been hunting for natural antioxidants for decades. The dietary-derived antioxidants are abundant in fruits, vegetables, essential oils, and so on.[16–18] One of the most representative antioxidants in food, chlorogenic acid, is produced from crop plants, tea, and coffee beans,[19–21] and has been revealed various beneficial effects,

including anti-diabetes, anti-obesity, anti-inflammatory, and anti-FA peroxidation.[22,23] It is of our interest that chlorogenic acid prevents hepatic TG accumulation, and that chlorogenic acid possesses remarkable radical scavenging capacity.[24] However, the effect of chlorogenic acid on the physicochemical property of LDs is unavailable. The similar situation is found in another phenolic antioxidant isolated from the Pacific oyster, 3,5-dihydroxy-4-methoxybenzyl alcohol (DHMBA).[25] Different from chlorogenic acid, DHMBA activates nuclear factor erythroid 2-related factor 2 (Nrf2) pathway in hepatocytes, not only exerting ROS scavenging.[26] Activation of Nrf-2 pathway induces a battery of Nrf2-dependent genes and enzymes, such as phase II enzymes, xenobiotic transporters, and drug-metabolizing enzymes against ROS,[24,26,27] and then attenuates hepatic steatosis, insulin resistance, obesity, and inflammation in non-alcoholic steatohepatitis (NASH)-model mice.[28] However, the effect of DHMBA on the physicochemical property of LDs remains to be clarified, similar to the case of chlorogenic acid.

Therefore, here we aim to establish a novel fluorescence-based method for characterizing the LDs in number, size distribution, and degree of oxidation in human hepatocytes. There, two fluorescent probes are used to analyze intact and oxidized LDs individually. TG hydroperoxides (TG-OOH) are determined in hepatocytes by LC-

MS/MS to compare with the proposed method. The above information will show the difference between the effects of chlorogenic acid and DHMBA on LDs.

2. Materials and Methods

2.1 Chemicals

SRfluor 680-phenyl, a fluorescence probe for neutral lipids, was purchased from Funakoshi Co. Ltd. (Tokyo, Japan). Liperfluo and Hoechst33342, fluorescence probes for lipid peroxides and nuclei, respectively, were purchased from Dojindo Laboratories (Kumamoto, Japan). LC-MS grade chloroform, isopropanol, methanol, and water were purchased from Wako Pure Chemical (Osaka, Japan). Ammonium formate, ammonium acetate, and butylated hydroxytoluene (BHT) were obtained from Sigma-Aldrich (St. Louis, MO). The free fatty acids, namely palmitic acid (PA), oleic acid (OA), and linoleic acid (LA) were purchased from Cayman Chemical Co. (Ann Arbor, MI). 2,2'-Azobis(2-amidinopropane) dihydrochloride (AAPH) (oxidant) and chlorogenic acid (antioxidant) were purchased from Sigma-Aldrich. DHMBA was chemically synthesized in house as previously reported.[25] Other chemicals and reagents were of analytical grade and purchased from Kanto Chemical Industry (Tokyo, Japan) unless specified.

106 **2.2 Cell culture**

107 Human HepG2 cells were cultured in DMEM supplemented with 10% FBS, 0.225%
108 $NaHCO_3$, 100 mg/mL penicillin, and 100 U/mL streptomycin at 37°C under 5% CO_2. For
109 this experiment, 35 mm glass bottom dish (MATSUNAMI, Japan) was coated with 0.1%
110 gelatin solution for 30 min at room temperature. The cells were cultured in 0.1% gelatin-
111 coated glass bottom dishes with 6×10^5 cells in 3 mL of the medium. After a 24-hour
112 incubation, the cells were treated with 400 μM free FAs and 1 mM AAPH (pro-oxidant)
113 or antioxidants (0–500 μM DHMBA or chlorogenic acid).

114 **2.3 Fluorescence imaging parameters**

115 Cells were washed in PBS, and then stained with 5 μM SRfluor 680-phenyl, 10 μM
116 Liperfluo, and 10 μg/mL Hoechst33342 for 30 min at 37°C. After incubation, the staining
117 buffer was replaced with serum free DMEM. Fluorescence was observed using the BZ-
118 9000 fluorescence microscope (Keyence Co. Ltd., Osaka, Japan) equipped with the
119 following filter sets; excitation: 360/40 nm, emission: 460/50 nm, dichroic mirror: 400
120 nm (blue); excitation: 470/40 nm, emission: 525/50 nm, dichroic mirror: 495 nm (green);
121 excitation: 620/60 nm, emission: 700/75 nm, dichroic mirror: 660 nm (red). Each
122 fluorescence were observed following fluorescence acquisition parameters:
123 Hoechst33342 fluorescence (excitation: 350 nm, emission: 361 nm, acquisition time:

200 milliseconds, binning: 2 × 2, F-stop: 1, field-of-view: 100 μm × 100 μm); Liperfluo fluorescence (excitation: 487−524 nm, emission: 535−579 nm, acquisition time: 770 milliseconds, binning: 2 × 2, F-stop: 1, field-of-view: 100 μm × 100 μm); SRfluor fluorescence (excitation: 615−650 nm, emission: 695−770 nm, acquisition time: 300 milliseconds, binning: 2 × 2, F-stop: 1, field-of-view: 100 μm × 100 μm).[29–31] Three to five visual field were randomly selected per dish, and bright field and three fluorescence images (blue, green, and red) were obtained from each same visual field.

2.4 LC/MS analysis

Lipids were extracted from the cultured cells according to Folch et al.[32] In brief, the cells were extracted with 600 μL of ice-cold chloroform/methanol 2:1 (*v/v*, with 0.002% BHT and TG 11:0/11:0/11:0 as internal standard) twice, and then dried in vacuum. The residues were dissolved in 100 μL of methanol, and then centrifuged at 680 *g* under 4°C for 15 min to remove any insoluble materials, and thereafter stored at −80°C until analysis. All procedures were finished within 1 hour to avoid lipid degradation and auto-oxidation.

The lipid extracts were injected into a Shimadzu Prominence HPLC system (Shimadzu Corp., Kyoto, Japan) coupled to an LTQ Orbitrap mass spectrometer (Thermo Fisher Scientific Inc., Waltham, MA) under ESI-positive mode. The detail parameters are shown in supplementary material. The extracted ion chromatograms (EICs) were drawn within

the mass tolerance of 5.0 ppm, and the LC/MS identification of lipid molecules were on the basis of their HRMS data compared with our in-house library,[33,34] as well as their retention behavior on the reversed-phase LC column. Peak extraction, EIC peak area integration, and semi-quantitation from the raw data were utilized by Xcalibur 2.2 (Thermo-Fisher Scientific Inc.).

2.5 Statistical analysis

In all experiments, cells were cultured 3 dishes for each group. All the data were analyzed by one-way ANOVA followed by Dunnett's multiple comparison test and expressed as means ± SD. *P* values less than 0.05 were considered to be statistically significant.

3 Results and Discussion

3.1 The workflow of intact and oxidized LD imaging analyses

The scheme for image analysis is shown in **Fig. 1**. Acquired images were analyzed by ImageJ 1.50i software.[35,36] To calibrate the length in ImageJ, pixel length of scale bar in the same magnification image was measured by using "Measure" command. SRfluor and Liperfluo fluorescence, and bright field images were obtained (**Figs. 1-A1**, **B1**, and **C1**), and then binarized based on the threshold set with reference to "RenyiEntropy" operation (**Figs. 1-A2**, **B2**, and **C2**). To exclude non-specific fluorescence and also to obtain the

positive image of oxidized LDs (oxLDs), an intersectional image was obtained from binarized images of bright field, SRfluor, and Liperfluo in the same visual field by using "Add" operation in Image Calculator of ImageJ (**Figs. 1-A2**, **B2**, **C2**, and **D**). To obtain an image of non-oxidized LDs (non-oxLDs), **Fig. 1-C2** was inverted by using "Invert" command (**Fig. 1-C3**), and an intersectional image was obtained from the images shown in **Figs. 1-A2**, **B2**, and **C3** by using "Add" operation (**Fig. 1-E**).

To obtain the number of oxLDs and non-oxLDs, the images (**Figs. 1-D** and **E**) were analyzed using "Analyze Particles" command. The images obtained with Hoechst33342 of the same visual field were also binarized and analyzed using "Analyze Particles". The number of nuclei was used for normalization of oxLDs and non-oxLDs as the number of cells. According to Wang et al.[2] and Cohen et al.[37], LDs smaller than 3 μm^2 and those not less than 3 μm^2 were defined as small and large LDs, respectively. The number of LD was defined as the sum of the numbers of non-oxLDs and oxLDs.

3.2 Evaluation of oxidation in the FA-induced LDs

3.2.1 Effects of FAs in the presence of AAPH

LDs were induced in the HepG2 cells by PA, OA, or LA in the presence of AAPH (positive control). The fluorescence images for the PA-loaded cells are shown in **Fig. 2-A**. The number of LDs and oxLDs significantly increased at 48 h ($P < 0.01$) (**Figs. 2-B1**

178 and **B2**). The degree of LD oxidation as estimated by the oxLD/LD ratio was significantly
179 increased at 8 h in small LDs (16.2 ± 4.5%) and at 24 h in large LDs (74.2 ± 7.6%)
180 (**Fig. 2-B3**). In the OA-loaded cells (**Fig. 3-A**), a significant increase was observed in the
181 numbers of small LDs and small oxLDs at both 24 h *(P* < 0.001) and 48 h (*P* < 0.01),[7,29]
182 and in the numbers of large LDs and large oxLDs at 48 h (*P* < 0.05) (**Figs. 3-B1** and **B2**).
183 The degree of LD oxidation in small and large LDs significantly increased at both 24 h
184 (62.8 ± 4.4% and 94.7 ± 2.7%) and 48 h (46.7 ± 9.4% and 89.1 ± 11.1%) (*P* < 0.001)
185 (**Fig. 3-B3**). In the LA-loaded cells, a significant increase was observed in the numbers
186 of small LDs at 24 h (*P* < 0.05) and small oxLDs at 48 h (*P* < 0.001), and in the numbers
187 of large LDs at 24 h (*P* < 0.05) and large oxLDs at 48 h (*P* < 0.001) (**Figs. 4-B1** and **B2**).
188 The degree of LD oxidation significantly increased in small LDs at 48 h (50.0 ± 15.9%)
189 (*P* < 0.001) and in large LDs at both 24 h (41.5 ± 15.9%) (*P* < 0.01) and 48 h
190 (86.9 ± 6.0%) (*P* < 0.001) (**Fig. 4-B3**).

191 The LC/MS characteristics of the TG-OOH species are listed in **Table S1 of**
192 **Supplementary Materials**. The cellular levels of these TG-OOH species are listed in
193 **Table S2**. Changes of total TG-OOH in the cells treated with FAs in the presence of
194 AAPH are compared (**Figure 5)**. In the PA- and OA-loaded cells, total TG-OOH
195 significantly increased at 24 h (10.3 ± 0.7 fold and 23.94 ± 10.4 fold vs. 0 h) (**Figs. 5-A**

196 and **B**), and then remarkably decreased at 48 h. On the other hand, in the LA-loaded cells,
197 TG-OOH significantly and strikingly increased at 48 h (215.3 ± 27.3 fold vs. 0 h) (**Fig.**
198 **5-C**).

199 Liperfluo is reported to react specifically with lipid peroxides and to be useful in
200 detection of intracellular lipid peroxides.[30,31] TG is a less polar lipid, and therefore, is
201 located in the core of LDs in cell. Further, in our proposed method, the signal of Liperfluo
202 came from lipid hydroperoxide in LDs, since non-specific signals had been excluded in
203 the process of intersection (**Fig. 1-D**). Moreover, the increase of TG-OOH also supported
204 this assumption: the significant increase of TG-OOH in the OA- and LA-loaded cells (**Fig.**
205 **5**) was associated with the significant increase of small oxLDs (**Figs. 3-B2** and **4-B2**).

206 **3.2.2 Effects of FAs in the absence of AAPH**

207 In the LA-loaded cells (**Fig. S1-C**), a significant increase was observed in the numbers of
208 small LDs at 4 h - 48 h ($P < 0.01$) and of small oxLDs at 8 h - 48 h ($P < 0.01$), and in the
209 numbers of large LDs and large oxLDs at 8 h - 48 h ($P < 0.05$) (**Figs. 6-C1** and **C2**). The
210 degree of LD oxidation in small and large LDs significantly increased at 4 h - 48 h
211 (25.6 ± 6.6% - 38.0 ± 3.4% and 52.3 ± 21.7% - 72.2 ± 12.4%) ($P < 0.01$) (**Fig. 6-C3**).
212 Although the similar trend was observed in the PA- and OA-loaded cells (**Figs. 6-A** and
213 **B**), the process proceeded more slowly than that in the LA-induced cells (**Fig. 6-C**).

It is of interest that the LA-induced LDs were oxidized the most slowly among the three FAs in the presence of AAPH, but the most quickly in the absence of AAPH (**Figs. 2, 3, 4,** and **6**). To explain this discrepancy, we speculate that the LA incorporated in the LA-induced LDs as TG served as a reservoir of oxidative stress caused by AAPH. On the other hand, in the absence of AAPH, the higher desaturation in LA than that in PA and OA might have resulted in the increased susceptibility of the LA-induced LDs to oxidation (**Figs. 6-A3**, **B3**, and **C3**). On the basis of these findings, LD oxidation seems to depend on both the fatty acyl composition of TG and the strength of oxidative stress.[38]

According to the present study, LDs can be oxidized in the cells, and therefore, can initiate and promote radical chain reactions. Moreover, LDs can provide fuels to continue the reactions, which results in intense, prolonged, and expanding oxidative reactions in the cells. Hence, it is highly possible that the LD-involved radical chain reaction exhausts the cellular antioxidant system, causing irreversible damages to the cell. A previous study reported that NAFLD model rats experienced complications with chronic depletion of hepatic glutathione (GSH), leading to a decrease of ROS scavenging activity.[39]

3.3 Evaluation of the effects of food-derived antioxidants on LDs by the proposed method

Because of the high susceptibility of the LA-induced LDs to oxidation (**Fig. 6-C**), we

232 investigated the effects of antioxidants on the LA-induced LDs in the absence of AAPH.
233 DHMBA represents indirect antioxidants, and chlorogenic acid represents direct
234 antioxidants.[27] Their structures are shown in **Fig. 7**. DHMBA decreased both the number
235 of oxLDs and the degree of oxidation (**Fig. 8-A**). On the other hand, chlorogenic acid
236 decreased large LDs and large oxLDs (**Figs. 8-B1 and B2**). However, it did not decrease
237 the degree of LD oxidation (**Fig. 8-B3**). The discrepancy in the effect on LDs between
238 the two compounds might be explained by their different antioxidative mechanisms.
239 DHMBA has been reported to protect hepatocytes *in vitro* from oxidative stress,[40] and
240 improve pathological and metabolic changes in the liver of NASH model mice.[28] The
241 increased expression of quinone reductase and glutathione reductase, induced *via*
242 activation of Nrf2 pathway by sulforaphane, are reported to maintain for more than 120
243 hours.[41] Thus, in our present study, DHMBA reduced the degree of oxidation in LDs
244 possibly through the activation of Nrf2-pathway (**Figs. 8-A2** and **A3**). Chlorogenic acid,
245 on the other hand, serves as a direct antioxidant exerting radical scavenging activity.[24,26]
246 Although the radical scavenging activity of chlorogenic acid is 3.1-fold stronger than that
247 of DHMBA,[26] the radical scavenging activity of direct antioxidants finish quickly due to
248 the oxidation of themselves.[42] In addition, chlorogenic acid suppresses fatty acid synthesis
249 and enhance β-oxidation.[40,43] Thus, in this study, chlorogenic acid decreased the number

of large LDs and oxLDs possibly through TG hydrolysis rather than antioxidative effects (**Figs. 8-B1** and **B2**). The proposed method could be a useful tool for future research on the interaction between antioxidants and LDs.

It should be noted that the present study has mainly technical aspect, however LD metabolism is concerned with ROS, ER stress, mitochondrial function, and lipogenic and lipolytic enzymes,[44,45] which might be also involved in LD oxidation. It is expected to get a better understanding of LD metabolism that clarification of the detailed interaction among the oxidation of LDs, ROS, ER stress, and mitochondrial function. For another limitation, the result with primary cells might be different from those with the cultured tumor cells,[46] like HepG2 cell used in the present study. Thus, the present method might not perfectly represent the physiological conditions in liver. Although the difference of the result between primary cells and HepG2 cells should be verified in the future, HepG2 cells are more suitable for stable screening of antioxidants than primary cells, because HepG2 is readily available and easy to grow. Thus, our proposed method using HepG2 cells could promise the utility as a globally usable method.

In conclusion, the proposed imaging method can provide detailed physicochemical information of LDs in hepatocytes. This method might be useful to explore antioxidant foods and drugs for prevention and alleviation of health disorders involving LD

accumulation and lipid oxidation.

Abbreviations Used

AAPH, 2,2'-azobis (2-amidinopropane) dihydrochloride; BHT, butylated hydroxytoluene; LA, linoleic acid; LC, liquid chromatography; LD, lipid droplet; MS, mass spectrometry; NAFLD, non-alcoholic fatty liver disease; OA, oleic acid; oxLD, oxidized lipid droplet; PA, palmitic acid; PC, phosphatidylcholine; ROS, reactive oxygen species, TG, triglyceride; TG-OOH, triglyceride hydroperoxide.

Acknowledgment

This research was supported by Encouraged research expenses to Takayuki Tsukui in Sapporo University of Health Sciences. The authors also thank Central Research Laboratory, Faculty of Health Sciences, Hokkaido University, for kindly providing the work space and instrument.

Supporting Information

LC/MS data of the identified triacylglycerol hydroperoxides and their relative intensities are listed in the Supplementary Materials.

Conflict of interest

The authors declare no competing financial interests.

References

(1) Olzmann, J. A.; Carvalho, P. Dynamics and Functions of Lipid Droplets. *Nat. Rev. Mol. Cell Biol.* **2019**, *20* (3), 137–155.

(2) Wang, H.; Wei, E.; Quiroga, A. D.; Sun, X.; Touret, N.; Lehner, R. Altered Lipid Droplet Dynamics in Hepatocytes Lacking Triacylglycerol Hydrolase Expression. *Mol. Biol. Cell* **2010**, *21* (12), 1991–2000.

(3) Kuerschner, L.; Moessinger, C.; Thiele, C. Imaging of Lipid Biosynthesis: How a Neutral Lipid Enters Lipid Droplets. *Traffic* **2008**, *9* (3), 338–352.

(4) Prinz, W. A. A Bridge to Understanding Lipid Droplet Growth. *Dev. Cell* **2013**, *24* (4), 335–336.

(5) Wilfling, F.; Wang, H.; Haas, J. T.; Krahmer, N.; Gould, T. J.; Uchida, A.; Cheng, J.-X.; Graham, M.; Christiano, R.; Fröhlich, F.; et al. Triacylglycerol Synthesis Enzymes Mediate Lipid Droplet Growth by Relocalizing from the ER to Lipid Droplets. *Dev. Cell* **2013**, *24* (4), 384–399.

(6) Martin, S.; Parton, R. G. Lipid Droplets: A Unified View of a Dynamic Organelle.

304 *Nat. Rev. Mol. Cell Biol.* **2006**, *7* (5), 373–378.

305 (7) Brasaemle, D. L. Thematic Review Series: Adipocyte Biology . The Perilipin
306 Family of Structural Lipid Droplet Proteins: Stabilization of Lipid Droplets and Control
307 of Lipolysis. *J. Lipid Res.* **2007**, *48* (12), 2547–2559.

308 (8) Mehlem, A.; Hagberg, C. E.; Muhl, L.; Eriksson, U.; Falkevall, A. Imaging of
309 Neutral Lipids by Oil Red O for Analyzing the Metabolic Status in Health and Disease.
310 *Nat. Protoc.* **2013**, *8* (6), 1149–1154.

311 (9) Zhao, Y.; Chen, Z.; Wu, Y.; Tsukui, T.; Ma, X.; Zhang, X.; Chiba, H.; Hui, S.-P.
312 Separating and Profiling Phosphatidylcholines and Triglycerides from Single Cellular
313 Lipid Droplet by In-Tip Solvent Microextraction Mass Spectrometry. *Anal. Chem.* **2019**,
314 *91* (7), 4466–4471.

315 (10) Jin, Y.; Tan, Y.; Chen, L.; Liu, Y.; Ren, Z. Reactive Oxygen Species Induces Lipid
316 Droplet Accumulation in HepG2 Cells by Increasing Perilipin 2 Expression. *Int. J. Mol.*
317 *Sci.* **2018**, *19* (11), 3445.

318 (11) Sembongi, H.; Miranda, M.; Han, G.-S.; Fakas, S.; Grimsey, N.; Vendrell, J.;
319 Carman, G. M.; Siniossoglou, S. Distinct Roles of the Phosphatidate Phosphatases Lipin
320 1 and 2 during Adipogenesis and Lipid Droplet Biogenesis in 3T3-L1 Cells. *J. Biol. Chem.*
321 **2013**, *288* (48), 34502–34513.

(12) Nunn, A. D. G.; Scopigno, T.; Pediconi, N.; Levrero, M.; Hagman, H.; Kiskis, J.; Enejder, A. The Histone Deacetylase Inhibiting Drug Entinostat Induces Lipid Accumulation in Differentiated HepaRG Cells. *Sci. Rep.* **2016**, *6* (1), 28025.

(13) Nielsen, J.; Christensen, A. E.; Nellemann, B.; Christensen, B. Lipid Droplet Size and Location in Human Skeletal Muscle Fibers Are Associated with Insulin Sensitivity. *Am. J. Physiol. Metab.* **2017**, *313* (6), E721–E730.

(14) Browning, J. D.; Horton, J. D. Molecular Mediators of Hepatic Steatosis and Liver Injury. *J. Clin. Invest.* **2004**, *114* (2), 147–152.

(15) Goldberg, I. J.; Reue, K.; Abumrad, N. A.; Bickel, P. E.; Cohen, S.; Fisher, E. A.; Galis, Z. S.; Granneman, J. G.; Lewandowski, E. D.; Murphy, R.; et al. Deciphering the Role of Lipid Droplets in Cardiovascular Disease: A Report From the 2017 National Heart, Lung, and Blood Institute Workshop. *Circulation* **2018**, *138* (3), 305–315.

(16) Wolfe, K. L.; Kang, X.; He, X.; Dong, M.; Zhang, Q.; Liu, R. H. Cellular Antioxidant Activity of Common Fruits. *J. Agric. Food Chem.* **2008**, *56* (18), 8418–8426.

(17) Amorati, R.; Foti, M. C.; Valgimigli, L. Antioxidant Activity of Essential Oils. *J. Agric. Food Chem.* **2013**, *61* (46), 10835–10847.

(18) Song, W.; Derito, C. M.; Liu, M. K.; He, X.; Dong, M.; Liu, R. H. Cellular Antioxidant Activity of Common Vegetables. *J. Agric. Food Chem.* **2010**, *58* (11), 6621–

340 6629.

341 (19) Boettler, U.; Sommerfeld, K.; Volz, N.; Pahlke, G.; Teller, N.; Somoza, V.; Lang,
342 R.; Hofmann, T.; Marko, D. Coffee Constituents as Modulators of Nrf2 Nuclear
343 Translocation and ARE (EpRE)-Dependent Gene Expression. *J. Nutr. Biochem.* **2011**, *22*
344 (5), 426–440.

345 (20) Rababah, T. M.; Hettiarachchy, N. S.; Horax, R. Total Phenolics and Antioxidant
346 Activities of Fenugreek, Green Tea, Black Tea, Grape Seed, Ginger, Rosemary, Gotu Kola,
347 and Ginkgo Extracts, Vitamin E, and Tert -Butylhydroquinone. *J. Agric. Food Chem.*
348 **2004**, *52* (16), 5183–5186.

349 (21) Niggeweg, R.; Michael, A. J.; Martin, C. Engineering Plants with Increased
350 Levels of the Antioxidant Chlorogenic Acid. *Nat. Biotechnol.* **2004**, *22* (6), 746–754.

351 (22) Ohnishi, M.; Morishita, H.; Iwahashi, H.; Toda, S.; Shirataki, Y.; Kimura, M.;
352 Kido, R. Inhibitory Effects of Chlorogenic Acids on Linoleic Acid Peroxidation and
353 Haemolysis. *Phytochemistry* **1994**, *36* (3), 579–583.

354 (23) Naveed, M.; Hejazi, V.; Abbas, M.; Kamboh, A. A.; Khan, G. J.; Shumzaid, M.;
355 Ahmad, F.; Babazadeh, D.; FangFang, X.; Modarresi-Ghazani, F.; et al. Chlorogenic Acid
356 (CGA): A Pharmacological Review and Call for Further Research. *Biomed.*
357 *Pharmacother.* **2018**, *97*, 67–74.

(24) Dinkova-Kostova, A. T.; Talalay, P. Direct and Indirect Antioxidant Properties of Inducers of Cytoprotective Proteins. *Mol. Nutr. Food Res.* **2008**, *52 Suppl 1*, S128-38.

(25) Watanabe, M.; Fuda, H.; Jin, S.; Sakurai, T.; Ohkawa, F.; Hui, S.-P.; Takeda, S.; Watanabe, T.; Koike, T.; Chiba, H. Isolation and Characterization of a Phenolic Antioxidant from the Pacific Oyster (Crassostrea Gigas). *J. Agric. Food Chem.* **2012**, *60* (3), 830–835.

(26) Joko, S.; Watanabe, M.; Fuda, H.; Takeda, S.; Furukawa, T.; Hui, S.-P.; Shrestha, R.; Chiba, H. Comparison of Chemical Structures and Cytoprotection Abilities between Direct and Indirect Antioxidants. *J. Funct. Foods* **2017**, *35*, 245–255.

(27) Tumer, T. B.; Rojas-Silva, P.; Poulev, A.; Raskin, I.; Waterman, C. Direct and Indirect Antioxidant Activity of Polyphenol- and Isothiocyanate-Enriched Fractions from Moringa Oleifera. *J. Agric. Food Chem.* **2015**, *63* (5), 1505–1513.

(28) Watanabe, M.; Fuda, H.; Okabe, H.; Joko, S.; Miura, Y.; Hui, S.-P.; Yimin; Hamaoka, N.; Miki, E.; Chiba, H. Oyster Extracts Attenuate Pathological Changes in Non-Alcoholic Steatohepatitis (NASH) Mouse Model. *J. Funct. Foods* **2016**, *20*, 516–531.

(29) Rice, D. R.; White, A. G.; Leevy, W. M.; Smith, B. D. Fluorescence Imaging of Interscapular Brown Adipose Tissue in Living Mice. *J. Mater. Chem. B* **2015**, *3* (9), 1979–

376 1989.

377 (30) Kagan, V. E.; Mao, G.; Qu, F.; Angeli, J. P. F.; Doll, S.; Croix, C. S.; Dar, H. H.;

378 Liu, B.; Tyurin, V. A.; Ritov, V. B.; et al. Oxidized Arachidonic and Adrenic PEs Navigate

379 Cells to Ferroptosis. *Nat. Chem. Biol.* **2017**, *13* (1), 81–90.

380 (31) Yamanaka, K.; Saito, Y.; Sakiyama, J.; Ohuchi, Y.; Oseto, F.; Noguchi, N. A

381 Novel Fluorescent Probe with High Sensitivity and Selective Detection of Lipid

382 Hydroperoxides in Cells. *RSC Adv.* **2012**, *2* (20), 7894.

383 (32) Folch, J.; Lees, M.; Sloane Stanley, G. H. A Simple Method for the Isolation and

384 Purification of Total Lipides from Animal Tissues. *J. Biol. Chem.* **1957**, *226* (1), 497–509.

385 (33) Hui, S.-P.; Sakurai, T.; Takeda, S.; Jin, S.; Fuda, H.; Kurosawa, T.; Chiba, H.

386 Analysis of Triacylglycerol Hydroperoxides in Human Lipoproteins by Orbitrap Mass

387 Spectrometer. *Anal. Bioanal. Chem.* **2013**, *405* (14), 4981–4987.

388 (34) Shrestha, R.; Hui, S.-P.; Miura, Y.; Yagi, A.; Takahashi, Y.; Takeda, S.; Fuda, H.;

389 Chiba, H. Identification of Molecular Species of Oxidized Triglyceride in Plasma and Its

390 Distribution in Lipoproteins. *Clin. Chem. Lab. Med.* **2015**, *53* (11), 1859–1869.

391 (35) Abramoff, M. D.; Magalhães, P. J.; Ram, S. J. Image Processing with ImageJ.

392 *Biophotonics Int.* **2004**, *11* (7), 36–42.

393 (36) Schneider, C. A.; Rasband, W. S.; Eliceiri, K. W. NIH Image to ImageJ: 25 Years

394 of Image Analysis. *Nat. Methods* **2012**, *9* (7), 671–675.

395 (37) Cohen, B.-C.; Shamay, A.; Argov-Argaman, N. Regulation of Lipid Droplet Size
396 in Mammary Epithelial Cells by Remodeling of Membrane Lipid Composition—A
397 Potential Mechanism. *PLoS One* **2015**, *10* (3), e0121645.

398 (38) Ricchi, M.; Odoardi, M. R.; Carulli, L.; Anzivino, C.; Ballestri, S.; Pinetti, A.;
399 Fantoni, L. I.; Marra, F.; Bertolotti, M.; Banni, S.; et al. Differential Effect of Oleic and
400 Palmitic Acid on Lipid Accumulation and Apoptosis in Cultured Hepatocytes. *J.*
401 *Gastroenterol. Hepatol.* **2009**, *24* (5), 830–840.

402 (39) Kloek, J. J.; Maréchal, X.; Roelofsen, J.; Houtkooper, R. H.; van Kuilenburg, A.
403 B. P.; Kulik, W.; Bezemer, R.; Nevière, R.; van Gulik, T. M.; Heger, M. Cholestasis Is
404 Associated with Hepatic Microvascular Dysfunction and Aberrant Energy Metabolism
405 Before and During Ischemia-Reperfusion. *Antioxid. Redox Signal.* **2012**, *17* (8), 1109–
406 1123.

407 (40) Watanabe, M.; Fuda, H.; Jin, S.; Sakurai, T.; Hui, S.-P.; Takeda, S.; Watanabe,
408 T.; Koike, T.; Chiba, H. A Phenolic Antioxidant from the Pacific Oyster (Crassostrea
409 Gigas) Inhibits Oxidation of Cultured Human Hepatocytes Mediated by Diphenyl-1-
410 Pyrenylphosphine. *Food Chem.* **2012**, *134* (4), 2086–2089.

411 (41) Gao, X.; Dinkova-Kostova, A. T.; Talalay, P. Powerful and Prolonged Protection

412 of Human Retinal Pigment Epithelial Cells, Keratinocytes, and Mouse Leukemia Cells
413 against Oxidative Damage: The Indirect Antioxidant Effects of Sulforaphane. *Proc. Natl.*
414 *Acad. Sci. U. S. A.* **2001**, *98* (26), 15221–15226.
415 (42) Takebayashi, J.; Tai, A.; Yamamoto, I. Long-Term Radical Scavenging Activity
416 of AA-2G and 6-Acyl-AA-2G against 1,1-Diphenyl-2-Picrylhydrazyl. *Biol. Pharm. Bull.*
417 **2002**, *25* (11), 1503–1505.
418 (43) Huang, K.; Liang, X.; Zhong, Y.; He, W.; Wang, Z. 5-Caffeoylquinic Acid
419 Decreases Diet-Induced Obesity in Rats by Modulating PPARα and LXRα Transcription.
420 *J. Sci. Food Agric.* **2015**, *95* (9), 1903–1910.
421 (44) Wang, K. Autophagy and Apoptosis in Liver Injury. *Cell Cycle* **2015**, *14* (11),
422 1631–1642.
423 (45) Fujii, J.; Homma, T.; Kobayashi, S.; Seo, H. G. Mutual Interaction between
424 Oxidative Stress and Endoplasmic Reticulum Stress in the Pathogenesis of Diseases
425 Specifically Focusing on Non-Alcoholic Fatty Liver Disease. *World J. Biol. Chem.* **2018**,
426 *9* (1), 1–15.
427 (46) Liu, P.; Wang, W.; Tang, J.; Bowater, R. P.; Bao, Y. Antioxidant Effects of
428 Sulforaphane in Human HepG2 Cells and Immortalised Hepatocytes. *Food Chem.*
429 *Toxicol.* **2019**, *128*, 129–136.

Figure captions

Figure 1. Scheme of the protocol for image analysis. Three types of images (A1, B1, and C1) were binarized based on the threshold set with reference to “RenyiEntropy” algorithm. In binarized images (A2, B2, and C2), white area means positive area of each fluorescent. By using Image Calculator of ImageJ to obtain intersectional image, a common white area for LD (A2), SRfluor (B2) and Liperfluo (C2) was obtained. An intersectional image was shown as the oxidized LDs (oxLDs) in image (D). C3 was inverted from C2 and shown as Liperfluo negative area. By using Image Calculator of ImageJ to obtain intersectional image, a common white area for LD (A2), SRfluor (B2) and Liperfluo negative (C3) was obtained. An intersectional image was shown as the non-oxidized LDs (non-oxLDs) in image (E). D and E were analyzed for the number of white area by ImageJ and shown as the number of oxLD and non-oxLD. Total LDs means the total of oxLDs and non-oxLDs, the total of the number of oxLDs and non-oxLDs were shown as the number of LDs.

Figure 2. Lipid accumulation and oxidation in HepG2 cells treated with PA. Cells were seeded in glass bottom dishes and treated with 400 μM PA and 1 mM AAPH. After

0–48 h of incubation, the cells were stained with SRfluor® 680 Phenyl (red; neutral lipids), Liperfluo (green; lipid peroxides), and Hoechst33342 (blue; nuclei). A: Fluorescence images were acquired using a fluorescence microscope. The scale bar shown in each image is 10 μm. B: quantification of the number of LDs and oxLDs, and the degree of LD oxidation as calculated by the ratio oxLD/LD. ImageJ software was used for quantification of fluorescence images. The results are presented as the number of LD (B1), the number of oxLD (B2), and degree of oxidation (B3) for small (< 3 μm^2) and large (≥ 3 μm^2) LDs. Columns and bars represent the mean ± SD (n = 3). **P* < 0.05, ***P* < 0.01, ****P* < 0.001.

Figure 3. Lipid accumulation and oxidation in HepG2 cells treated with OA. LD stains and data processing were done as described in the explanation of **Fig. 2**. Columns and bars represent the mean ± SD (n = 3). **P* < 0.05, ***P* < 0.01, ****P* < 0.001.

Figure 4. Lipid accumulation and oxidation in HepG2 cells treated with LA. LD stains and data processing were done as described in the explanation of **Fig. 2**. Columns and bars represent the mean ± SD (n = 3). **P* < 0.05, ***P* < 0.01, ****P* < 0.001.

Figure 5. Change fold of intracellular TG-OOH in the FA-loaded cells in the presence of AAPH. Cells were loaded 400 μM PA (A), OA (B), and LA (C) with 1 mM AAPH. After 0–48 h of incubation, the whole cell lipid was extracted. TG-OOH was detected by LC/MS which condition was described in material and method section. Columns and bars represent the mean ± SD (n = 3). *$P < 0.05$, **$P < 0.01$, ***$P < 0.001$.

Figure 6. Quantification of the number of LDs and oxLDs, and the degree of LD oxidation as calculated by the ratio oxLD/LD. Cells were treated with 400 μM PA (A1-3), OA (B1-3), and LA (C1-3) in the absence of AAPH. After fluorescence staining, the cells were observed using a fluorescence microscope. ImageJ software was used for quantification of fluorescence images. The results are presented as the number of LD (A1, B1, and C1), the number of oxLD (A2, B2, and C2), and degree of oxidation (A3, B3, and C3) for small (< 3 μm^2) and large (≥ 3 μm^2) LDs. Columns and bars represent the mean ± SD (n = 3). *$P < 0.05$, **$P < 0.01$, ***$P < 0.001$.

Figure 7. Lipid accumulation and oxidation in HepG2 cells treated with LA and antioxidants. Cells were seeded in glass bottom dishes and treated with 400 μM LA and 0, 125, 250 and 500 μM of the following antioxidants: DHMBA (A) and chlorogenic acid

(B). After 8 h of incubation, the cells were stained with SRfluor® 680 Phenyl (red), Liperfluo (green), and Hoechst33342 (blue). Fluorescence images were acquired using a fluorescence microscope. The scale bar shown in each image is 10 μm.

Figure 8. Effects of antioxidants on lipid accumulation and oxidation of LA-induced LDs in the absence of AAPH. Cells were treated with 400 μM LA and 0, 125, 250 and 500 μM of the following antioxidants: DHMBA (A) and chlorogenic acid (B). After fluorescence staining, the cells were observed using a fluorescence microscope. To quantify the number of LDs and oxLDs, fluorescence images were analyzed with ImageJ software. The results are presented as the number of LD (A1 and B1), the number of oxLD (A2 and B2), and degree of oxidation (A3 and B3) for small ($< 3\ \mu m^2$) and large ($\geq 3\ \mu m^2$) LDs. Columns and bars represent the mean ± SD (n = 3). $*P < 0.05$, $**P < 0.01$.

Figure graphics

Figure 1

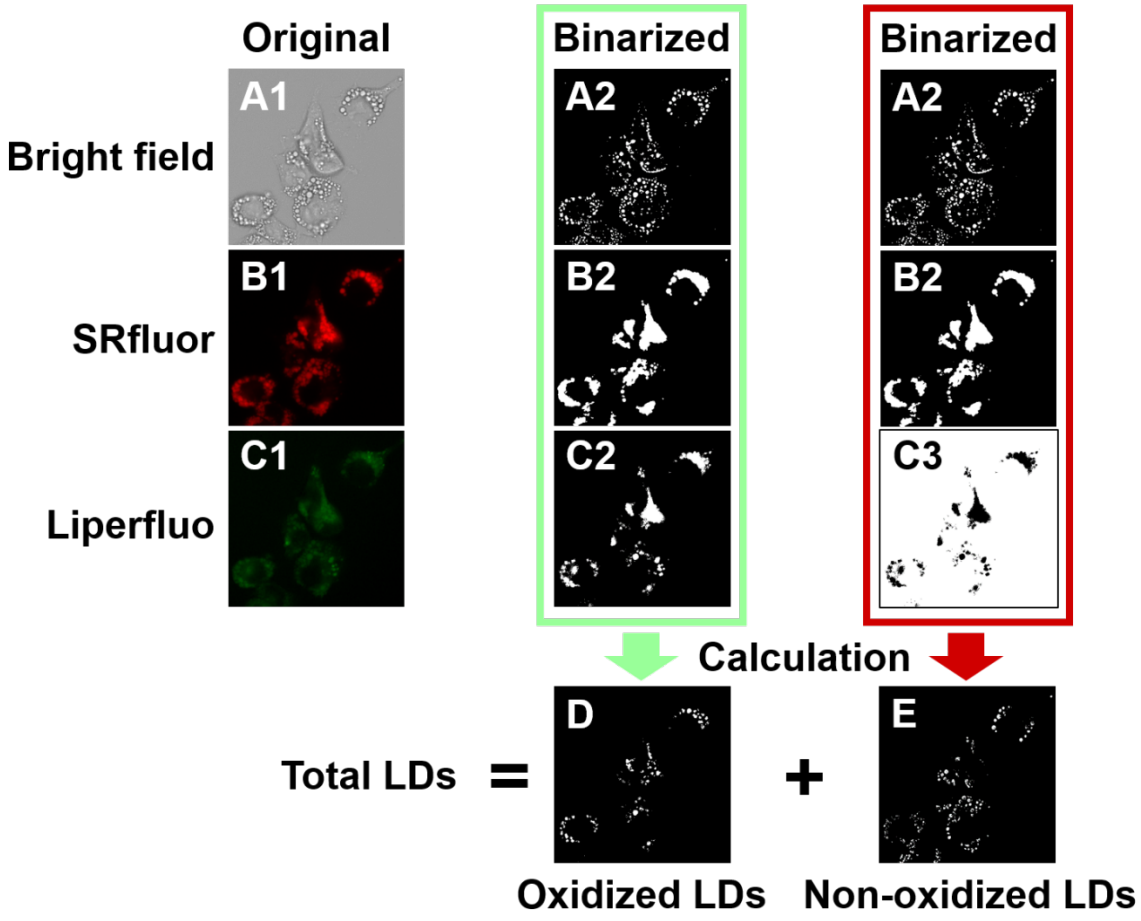

Figure 2

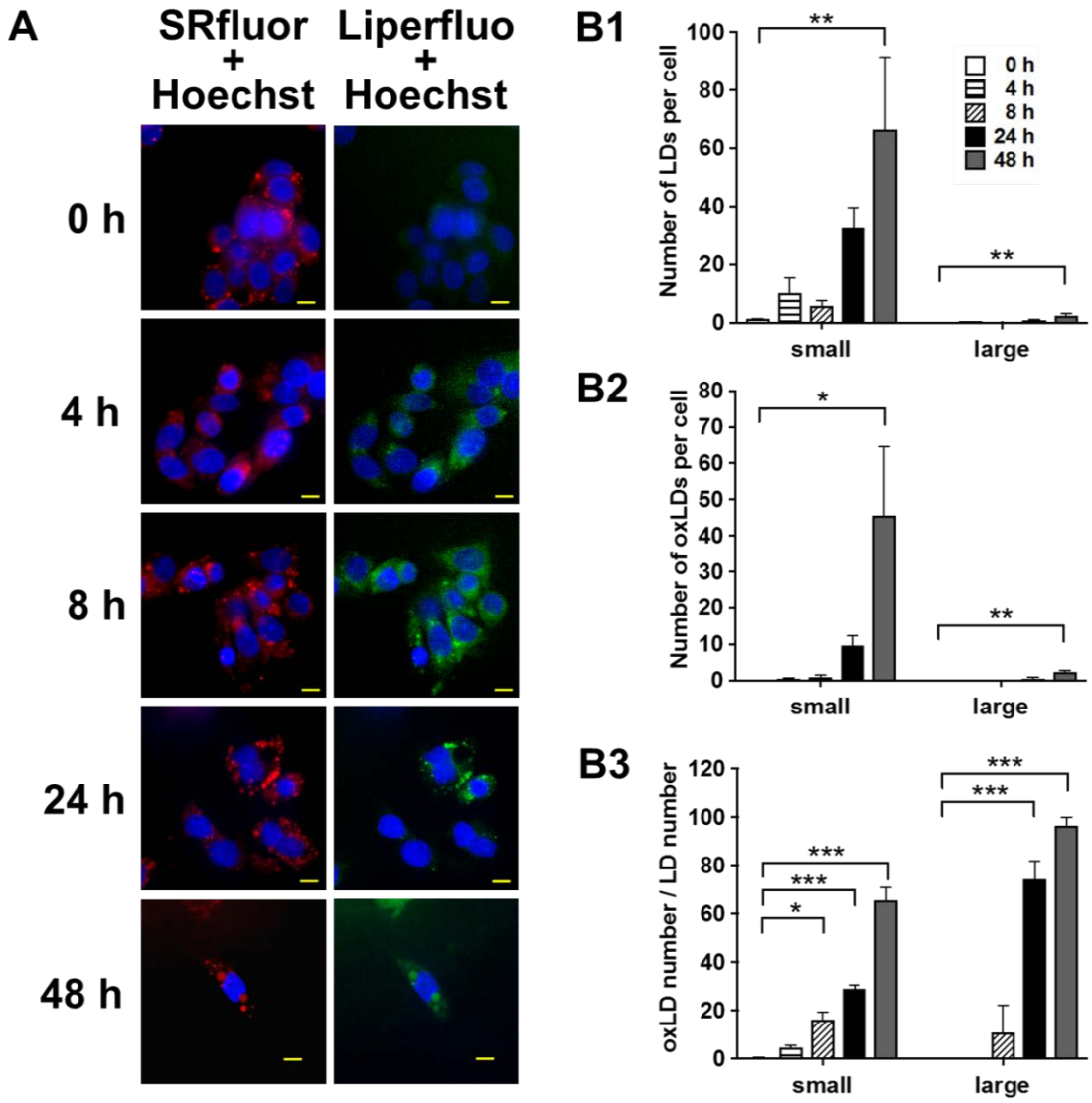
A
SRfluor + Hoechst
Liperfluo + Hoechst
0 h
4 h
8 h
24 h
48 h
B1
Number of LDs per cell
0 h
4 h
8 h
24 h
48 h
small
large
B2
Number of oxLDs per cell
small
large
B3
oxLD number / LD number
small
large

Figure 3

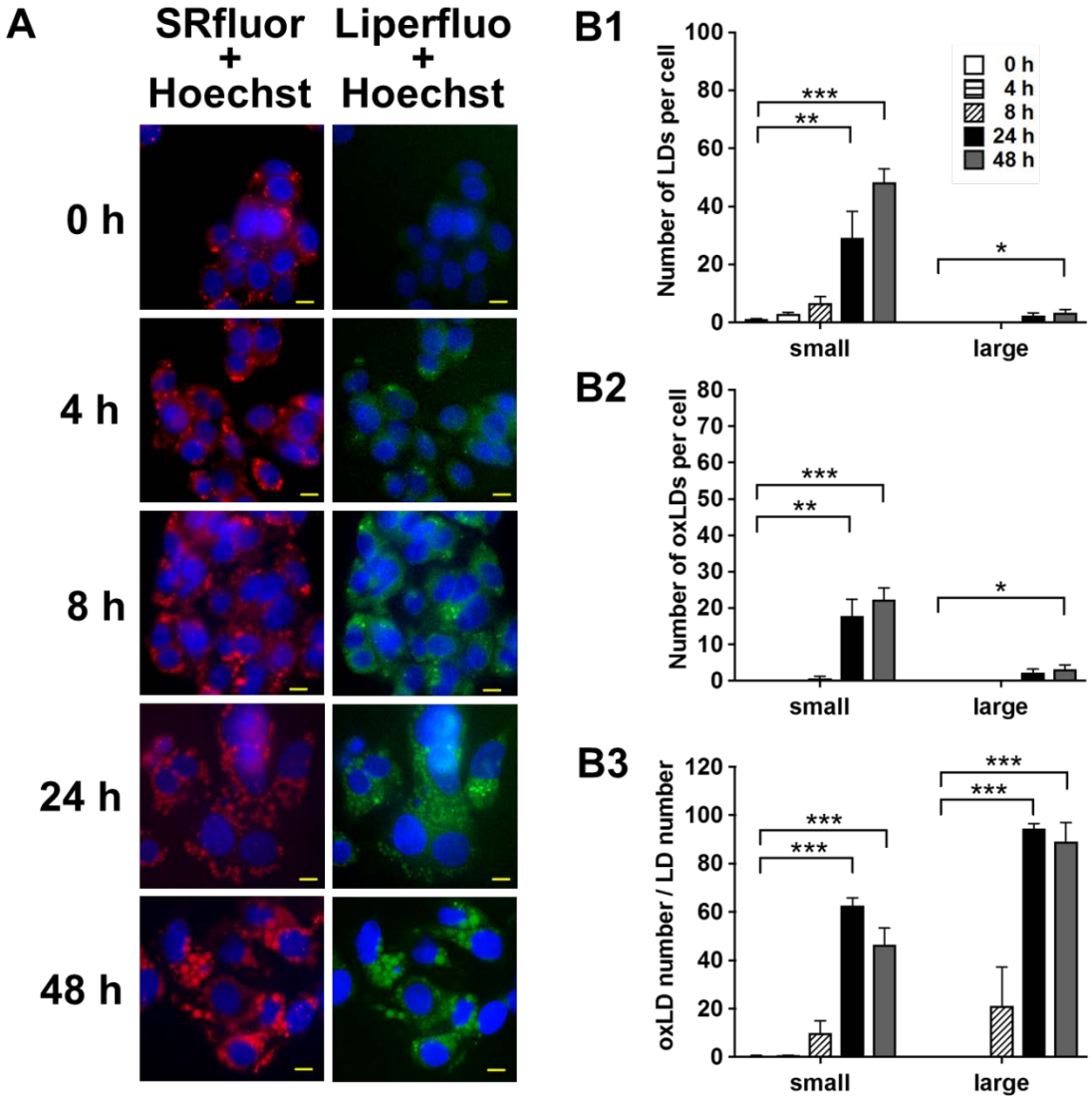
A
SRfluor + Hoechst
Liperfluo + Hoechst
0 h
4 h
8 h
24 h
48 h
B1
Number of LDs per cell
0 h
4 h
8 h
24 h
48 h
***
**
*
small
large
B2
Number of oxLDs per cell
***
**
*
small
large
B3
oxLD number / LD number
***
***
***
***
small
large

Figure 4

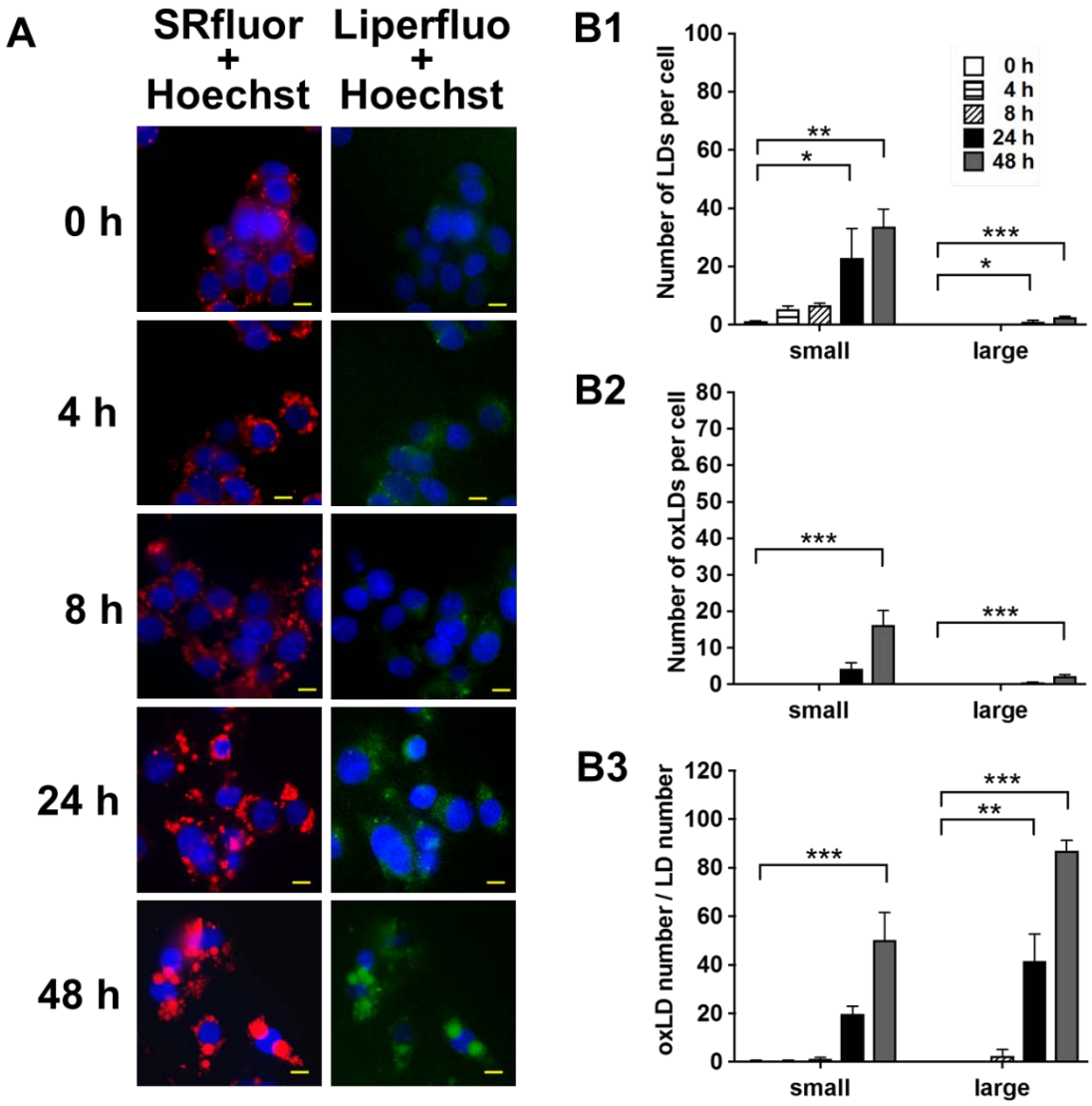
A
SRfluor + Hoechst
Liperfluo + Hoechst
0 h
4 h
8 h
24 h
48 h
B1
Number of LDs per cell
0 h
4 h
8 h
24 h
48 h
small
large
B2
Number of oxLDs per cell
small
large
B3
oxLD number / LD number
small
large

Figure 5

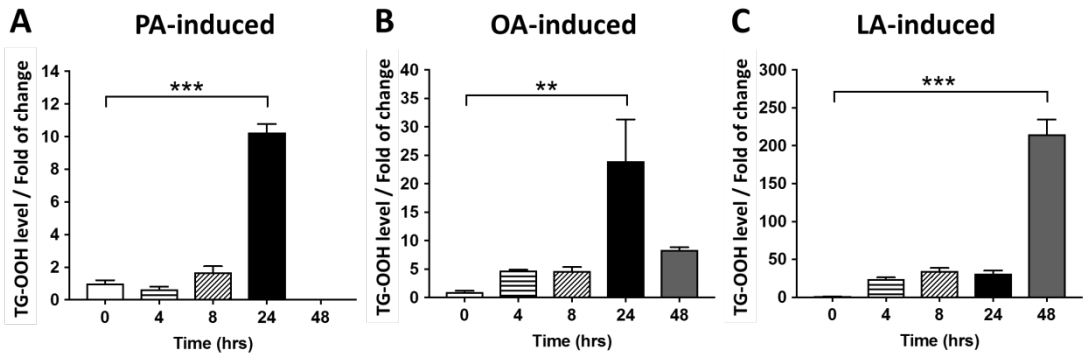
A
PA-induced
TG-OOH level / Fold of change
***
Time (hrs)
B
OA-induced
TG-OOH level / Fold of change
**
Time (hrs)
C
LA-induced
TG-OOH level / Fold of change
***
Time (hrs)

Figure 6

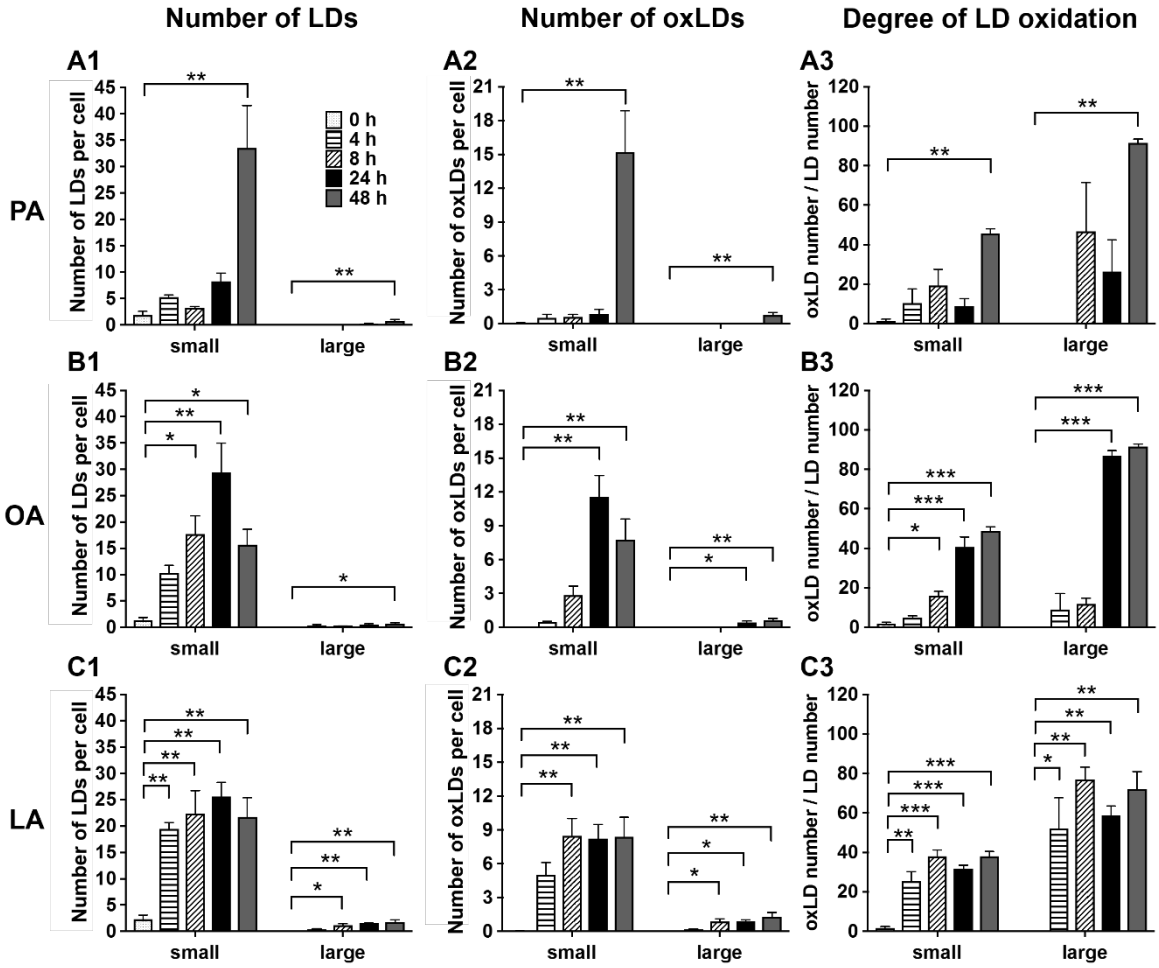
Number of LDs
Number of oxLDs
Degree of LD oxidation
A1
A2
A3
B1
B2
B3
C1
C2
C3
PA
OA
LA
Number of LDs per cell
Number of oxLDs per cell
oxLD number / LD number
0 h
4 h
8 h
24 h
48 h
small
large

Figure 7

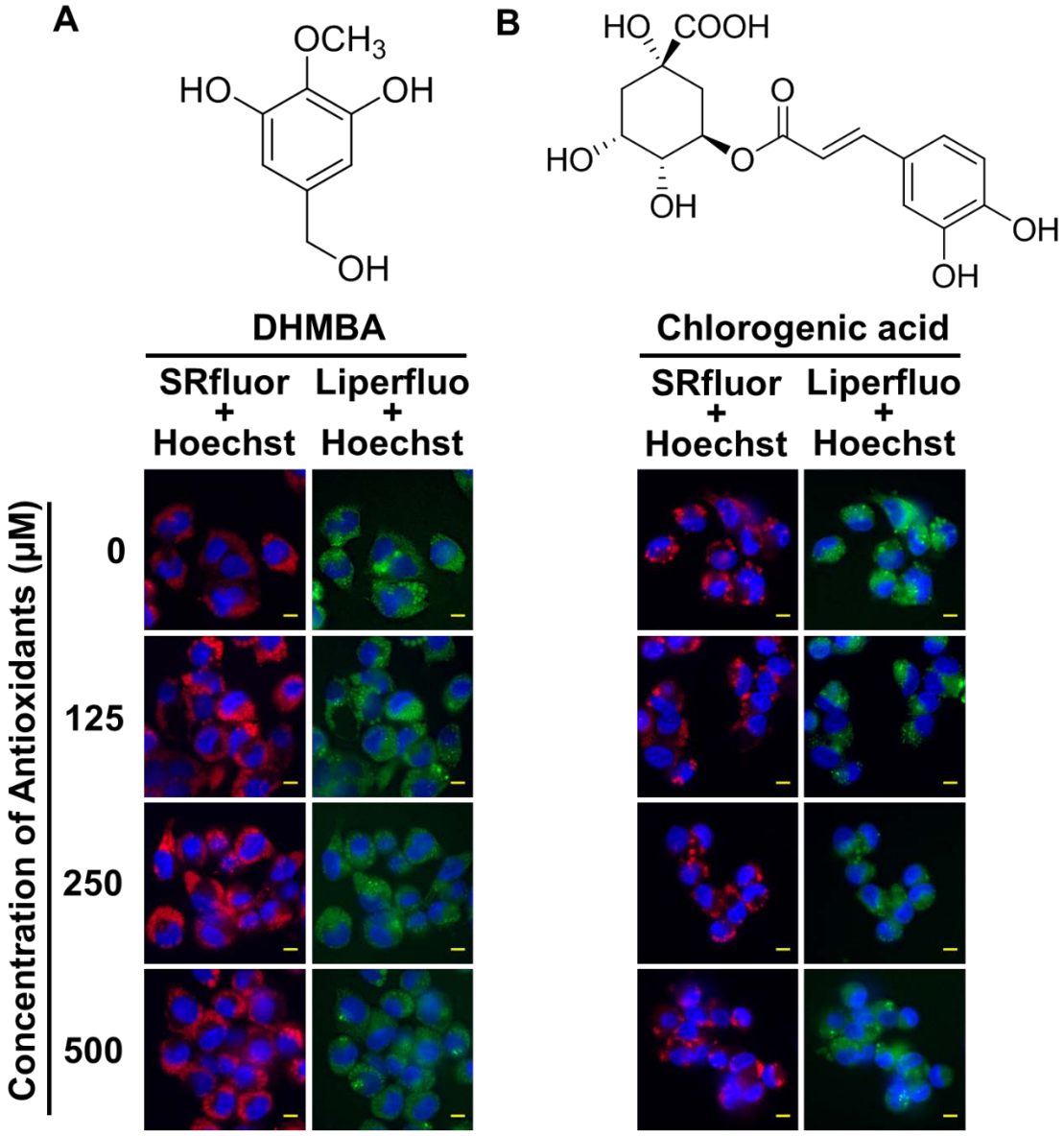
A
OCH3
HO
OH
OH
B
HO
COOH
O
HO
O
OH
OH
OH
DHMBA
Chlorogenic acid
SRfluor + Hoechst
Liperfluo + Hoechst
SRfluor + Hoechst
Liperfluo + Hoechst
Concentration of Antioxidants (μM)
0
125
250
500

Figure 8

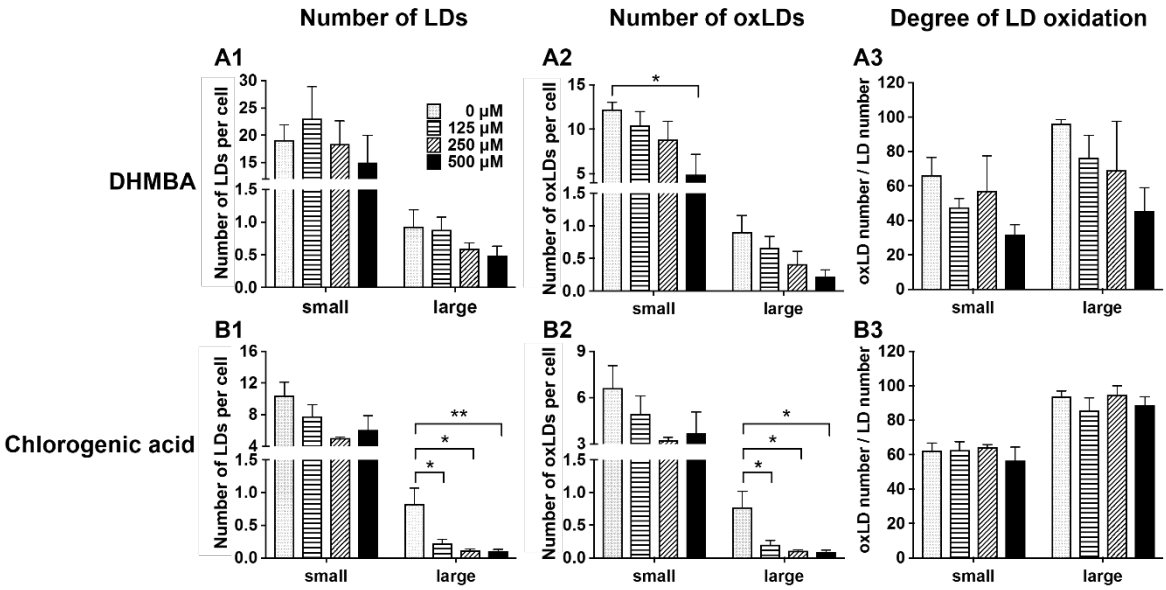
Number of LDs
Number of oxLDs
Degree of LD oxidation
A1
A2
A3
B1
B2
B3
DHMBA
Chlorogenic acid
Number of LDs per cell
Number of oxLDs per cell
oxLD number / LD number
0 µM
125 µM
250 µM
500 µM
small
large
*
**

Abstract Graphics